Analytical Biochemistry **273,** 284–290 (1999)
Article ID abio.1999.4223, available online at http://www.idealibrary.com on IDEAL®

Sequence-Dependent Conformational Differences of Small RNAs Revealed by Native Gel Electrophoresis

Penny J. Beuning,* Michael R. Tessmer,†,[1] Christoph G. Baumann,‡,[2] Deborah A. Kallick,† and Karin Musier-Forsyth*,[3]

**Department of Chemistry and †Department of Medicinal Chemistry, University of Minnesota, Minneapolis, Minnesota 55455; and ‡Department of Biochemistry, University of Minnesota, St. Paul, Minnesota 55108*

Received April 22, 1999

In this study, we use native polyacrylamide gel electrophoresis and one-dimensional NMR spectroscopy to analyze small RNA hairpins containing a UUCG tetraloop. The aggregation state of one RNA 16-mer (5′-CGGCUUCGGUCGACCA-3′) in the presence of Mg^{2+} was confirmed by laser light scattering. Although it is widely known in the RNA field that some RNAs tend to aggregate, especially when present at high concentrations, the sequence elements responsible for this effect are rarely identified. In this work, we show that Mg^{2+}-induced aggregation of the 16-mer RNA hairpin is sensitive to the presence of the 3′-terminal base and a specific 2′-hydroxyl group. Our study highlights the fact that even small changes in a particular RNA sequence can increase its tendency to undergo Mg^{2+}-dependent aggregation in an unpredictable manner. Our analysis also shows that native gel electrophoresis is a sensitive probe of RNA conformation with the capability to detect differences apparently caused by subtle base stacking effects at the ends of helices.

Key Words: **RNA; magnesium; native gel electrophoresis; laser light scattering; NMR.**

It is well established that divalent metal ions such as Mg^{2+} play an important role in the structure and folding of RNA. For this reason, it is of great interest to include metals in structural analyses of RNAs by solution NMR or X-ray crystallography. However, small sequence differences can induce rather significant conformational or topological changes in RNA in the presence of magnesium (1). We have observed this in our functional studies of small RNA helices that mimic the acceptor stem of tRNAs. In particular, as reported here, a single base pair transversion (5′-G:C to 5′-C:G) causes a dramatic change in the mobility of an RNA hairpin containing a UUCG tetraloop (16-mer) on both denaturing and native polyacrylamide gels, as well as significant broadening of the resonances revealed by NMR spectroscopy. Using laser light scattering, we confirmed that Mg^{2+}-dependent aggregation of the C:G RNA variant was responsible for the anomalous gel mobility and the appearance of the NMR spectra. Although it is widely known in the field of RNA research that some RNAs aggregate at high concentrations, careful documentation of the causes of aggregation is lacking in the literature. In the present work, we sought to identify specific sequence elements that are responsible for the apparent conformational heterogeneity induced by the base pair transversion. This analysis also shows that native gel electrophoresis is a useful probe of sequence-dependent conformational differences in small RNAs, including those caused by subtle stacking effects at the end of a helix.

MATERIALS AND METHODS

RNA Synthesis and Purification

RNA synthesis chemicals, the 2′-deoxyguanosine phosphoramidite, and the controlled pore glass solid supports were from Glen Research (Sterling, VA). All other RNA phosphoramidite monomers were purchased from Chemgenes (Waltham, MA). Ultrahigh purity acetonitrile and dichloroethane were obtained from J. T. Baker. $MgCl_2$ (99.995%) was from Aldrich. All buffers were prepared using diethylpyrocarbonate-

[1] Present address: Department of Chemistry, Southwestern College, 100 College St., Winfield, KS 67156.

[2] Present address: Department of Biology, University of York, Heslington, York Y01 5DD, United Kingdom.

[3] To whom correspondence should be addressed at Department of Chemistry, University of Minnesota, 207 Pleasant St. SE, Minneapolis, MN 55455. Fax: 612-626-7541. E-mail: musier@chem.umn.edu.

0003-2697/99 $30.00

treated water to reduce RNase contamination (2). RNA oligonucleotides were synthesized using the phosphoramidite method on a Gene Assembler Special (Pharmacia), deprotected, gel purified on denaturing 16% polyacrylamide–TBE gels, eluted, and desalted in the usual manner (3, 4). ^{32}P-end-labeled RNA was prepared using [γ-^{32}P]ATP according to a published procedure (2), purified on 16% polyacrylamide gels, and worked up in the same manner as unlabeled RNA. The RNA used for NMR analysis was further purified by extensive buffer exchange with the NMR buffer (100 mM NaCl, 10 mM $NaPO_4$, pH 6.2) using Centricon 3 concentrators (Amicon). The Centricons were prepared by shaking overnight at 250 rpm in the NMR buffer and then centrifuged with 1 mL NMR buffer at 6750*g* 15 times. RNA was then applied to the Centricons and washed first with 5 × 1 mL 0.1 M EDTA followed by 5 × 1 mL NMR buffer. The volume was reduced to 630 μL, D_2O was added to 700 μL final volume, the sample was annealed according to the procedure below, and was transferred to the NMR tube. RNA concentrations were determined using the following extinction coefficients: 9-mer, 8.90×10^4; 13-mer, 10.7×10^4; 14-mer, 11.5×10^4; 15-mer, 12.0×10^4; 16-mer, 13.0×10^4; 22-mer, 17.1×10^4 M^{-1} cm^{-1}.

Native Gel Electrophoresis

Native gel electrophoresis was carried out with 16% polyacrylamide–Tris–glycine–$MgCl_2$ gels at 4 or 20°C (2, 5). In some experiments $MgCl_2$ was omitted from the gel. RNA hairpin samples were annealed in 50 mM Hepes (pH 8.0) by heating at 80°C for 2 min, cooling to 60°C for 2 min, adding $MgCl_2$ to 10 mM, and cooling slowly to room temperature before finally placing them on ice. Equimolar amounts of each strand of RNA duplex samples were annealed in 50 mM Hepes (pH 8.0) by heating at 80°C for 2 min, cooling to 60°C for 2 min, adding $MgCl_2$ to 10 mM, and immediately placing them on ice. Immediately before loading onto the gel, glycerol was added to 40% final concentration. Unless otherwise indicated, 190–280 μM (20–30 μg in 20 μL) RNA was loaded per lane and bands were visualized by UV-shadowing. When autoradiography was used to visualize the RNA, ^{32}P-end-labeled RNA was combined with the appropriate concentration of unlabeled RNA before annealing.

Light Scattering

Laser light scattering experiments were performed using a Lexel Model 95-3 argon-ion laser operating at a wavelength of 488 nm and a power output of 100–250 mW. The laser beam was focused on a cylindrical scattering cell immersed in a thermostatically controlled oil bath. RNA samples were freshly annealed at a concentration of 410 μM in 50 mM NaCl and 10 mM $NaPO_4$ (pH 7.0) and passed through a 0.2-μm filter directly into acid-washed cells. Scattered light was detected with an ITT FW-130 photomultiplier tube at scattering angles of 30–90°. $MgCl_2$ was added from a 0.625 M stock. Apparent molecular weights were calculated using benzene as a reference scatterer. The refractive index increment was taken as 0.201 mL/g (6).

Nuclear Magnetic Resonance Spectroscopy

^{1}H NMR spectroscopy was performed either at 500 or 600 MHz on Varian Inova spectrometers. Observation of the imino protons was accomplished with the use of pulsed-field gradients. RNA samples contained 1 mM oligomer in 700 μL of 90% H_2O/10% D_2O buffer containing 100 mM NaCl, 10 mM $NaPO_4$ (pH 6.2) and 2.5 μM 2,2,3,3-tetradeuterio-3-trimethylsilylpropionic acid as a reference. The 16K spectra with 64 transients were routinely collected. Free induction decays were either transferred to a Silicon Graphics computer and analyzed using Felix 3.5 or transferred to a Sun workstation and analyzed using VNMR. Imino protons were assigned by comparison of data reported for similar sequences (7–10) and confirmed by the observation of interresidue NOEs as will be described in detail elsewhere.

RESULTS

Using model RNA duplex substrates that mimic the acceptor stem of $tRNA^{Ala}$, we previously showed that a single transversion at the terminal G:C base pair eliminated aminoacylation by alanyl-tRNA synthetase (11). Small RNA hairpins containing UUCG tetraloops are also substrates for alanyl-tRNA synthetase (Fig. 1, TL-I) (12), and a base pair transversion at position 1:12 eliminates aminoacylation (Fig. 1, TL-II). In the course of preparing large quantities of these small RNA hairpins for structural studies, we noticed that TL-I and TL-II had different electrophoretic mobilities even on a denaturing polyacrylamide gel. This result prompted us to use native gel electrophoresis to examine potential conformational differences between the two RNA samples. On a native polyacrylamide gel containing 190 μM (20 μg in 20 μL) RNA per lane and 10 mM $MgCl_2$ in both the gel and the running buffer, we observed a striking difference in the migration pattern of TL-I and TL-II (Fig. 2A). TL-I (G1:C12) migrates faster and runs as a single, compact band (Fig. 2A, lane 1), whereas TL-II (C1:G12) migrates as a smeared band significantly slower than TL-I (Fig. 2A, lane 2). We observe this difference regardless of whether electrophoresis is at 4 or 20°C. When similar amounts of TL-I and TL-II were electrophoresed on native gels in the

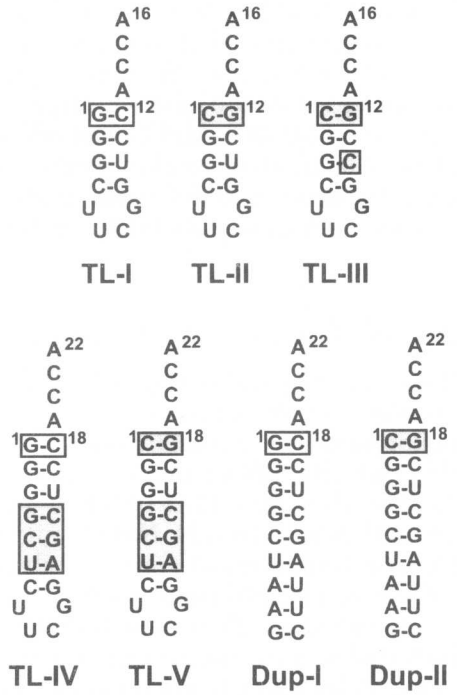

FIG. 1. The sequences of the chemically synthesized RNA hairpins and duplexes used in this study. The boxed base pair in TL-I indicates the position of interest in this study. All of the changes made in the RNA hairpins relative to TL-I are boxed and shaded. Dup-I and Dup-II are 9-base-pair duplexes derived from TL-IV and TL-V, respectively.

absence of $MgCl_2$, the two samples co-migrated (Fig. 2B). A similar result was obtained when the $MgCl_2$ in the gel was replaced with 15–30 mM NaCl (data not

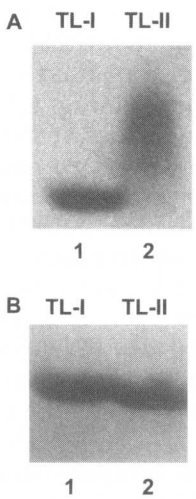

FIG. 2. Native polyacrylamide gel electrophoresis of the hairpin variants. Electrophoresis was at 4°C with 190 μM (20 μg in 20 μL) RNA loaded per lane. Lane 1, G1:C12 hairpin (TL-I); lane 2, C1:G12 hairpin (TL-II). (A) With 10 mM $MgCl_2$ in the gel and in the running buffer; (B) without $MgCl_2$. RNA was visualized by UV-shadowing.

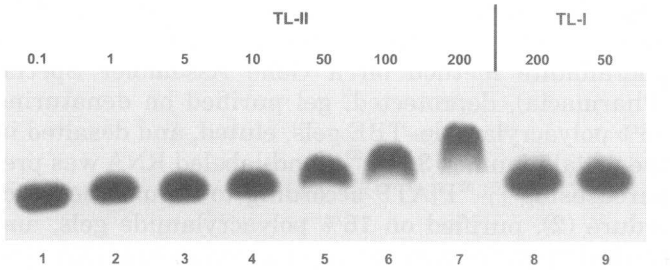

FIG. 3. Native polyacrylamide gel electrophoresis of varying concentrations of TL-I and TL-II. The ^{32}P-labeled RNAs were combined with nonradioactive RNA at the final concentrations indicated in a volume of 25 μL and annealed before electrophoresis in the presence of 10 mM $MgCl_2$ at 20°C. Lanes 1–7: TL-II at 0.1 μM (lane 1), 1 μM (lane 2), 5 μM (lane 3), 10 μM (lane 4), 50 μM (lane 5), 100 μM (lane 6), 200 μM (lane 7); lanes 8 and 9: TL-I at 200 μM (lane 8), 50 μM (lane 9). RNA was visualized by autoradiography.

shown). Therefore, the observed difference in gel mobility is Mg^{2+}-dependent, and a monovalent cation does not induce this effect. The retarded mobility and smeared appearance of the C1:G12-containing hairpin in the presence of Mg^{2+} suggests a significant degree of conformational heterogeneity and/or aggregation.

To assess the aggregation state of the species present in the smeared band observed for TL-II, we ^{32}P-end-labeled both TL-I and TL-II and electrophoresed samples of various concentrations (0.1 to 200 μM) on a native gel. We found that TL-II comigrated with TL-I at low concentrations (0.1 to 10 μM; Fig. 3, lanes 1–4), but that the gel mobility of TL-II decreased with increasing sample concentrations (50 to 200 μM; Fig. 3, lanes 5–7), behavior that is consistent with aggregation. In contrast, TL-I migrated as a single, compact band and was apparently a monomer at all concentrations examined (Fig. 3, lanes 8 and 9).

The conclusions from the native gel analysis were supported by solution NMR spectroscopy. The imino proton signals provide a convenient assay of base pairing, as each Watson–Crick base pair contributes one imino proton to the downfield region of the spectrum. The imino protons in the UUCG tetraloop are not normally observed (except occasionally at temperatures below 10°C and at pH values that minimize proton exchange). The imino proton spectra as a function of magnesium concentration are illustrated in Fig. 4. At all concentrations examined, Mg^{2+} has little effect on the appearance of the TL-I spectrum (Fig. 4A). We note that the resonances assigned to G1 and G2 are shifted slightly upfield in the presence of Mg^{2+}. Addition of Mg^{2+} to duplexes that resemble the top portion of TL-I was previously shown to result in small line-shift changes (8). This may be the due to the presence of a specific divalent metal binding site between the second and third base pairs (8, 13). For TL-II, each base-paired imino proton is observable at 0 mM Mg^{2+}. As the

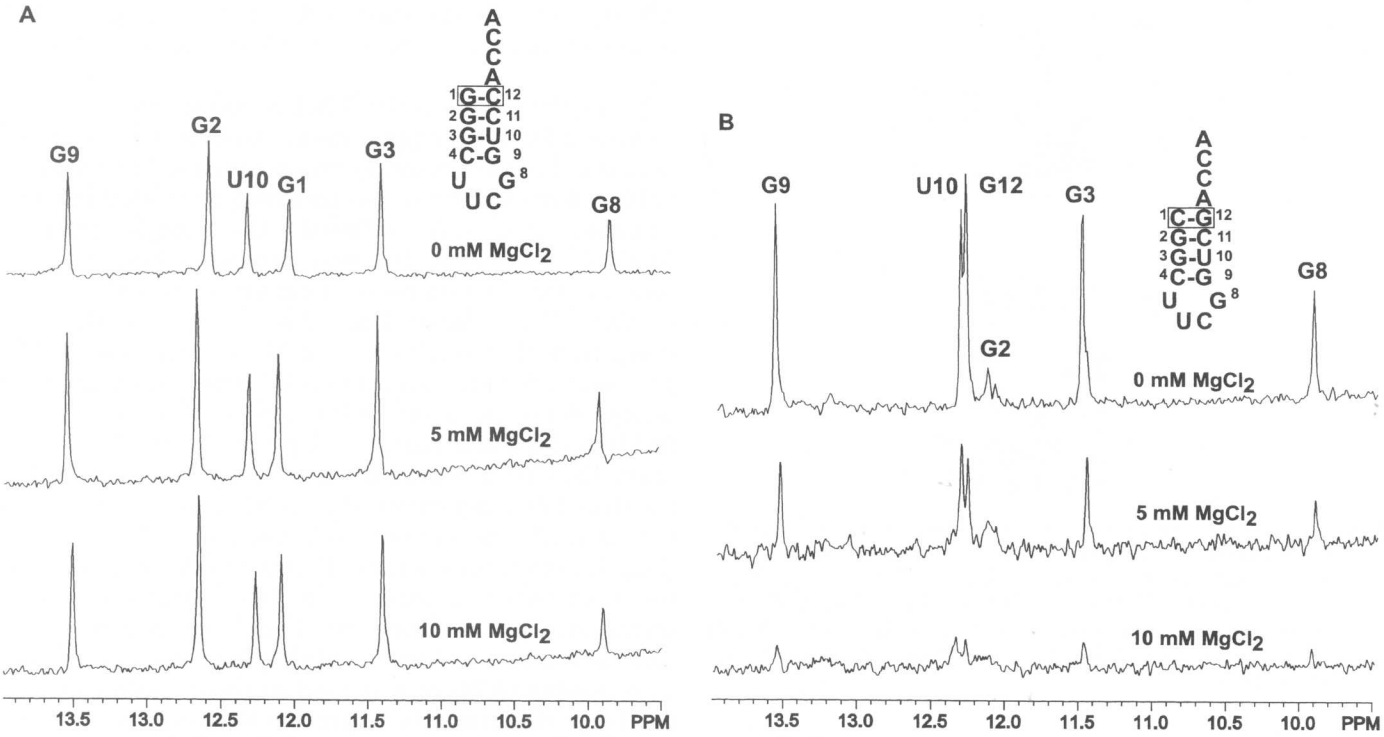

FIG. 4. The imino region of the proton NMR spectrum of TL-I and TL-II in the presence of varying amounts of Mg^{2+}. (A) The G1:C12 and (B) C1:G12 hairpins in the presence of 0 (top), 5 mM (middle), and 10 mM (bottom) $MgCl_2$.

concentration of Mg^{2+} increases, the imino proton peaks decrease in size and eventually (at 10 mM Mg^{2+}) nearly disappear (Fig. 4B). In the aromatic and ribose sugar regions of the TL-II spectra, most of the peaks are also broadened and/or significantly reduced in size. Therefore, the disappearance of the imino proton signals does not appear to signify unfolding of TL-II, but rather suggests that the molecular weight of the sample has increased beyond the detection limits of NMR. These spectra are consistent with the interpretation that Mg^{2+} induces aggregation of TL-II.

We also used laser light scattering to assess the aggregation state of the samples, and to try to quantify the number of RNAs associating in the slower migrating bands on the native gel shown in Fig. 2A. Figure 5 shows a plot of the intensity of scattered light for both RNA hairpins (410 μM) as a function of magnesium concentration. Our analysis of this data indicates that TL-I is a monomer at all Mg^{2+} concentrations examined (0–25 mM). However, the weight-average molecular weight of TL-II is slightly larger than the predicted molecular weight of a monomer at $Mg^{2+} \leq 2.5$ mM, about a "1.5-mer"; this RNA forms aggregates of increasing size at Mg^{2+} concentrations above 2.5 mM (Fig. 5). At 10 mM $MgCl_2$, conditions routinely employed in the native gel experiments, the light scattering data indicate that TL-II forms particles approximately four times the monomer molecular weight. Particles approximately eight times the monomer molecular weight are present when the concentration reaches 25 mM $MgCl_2$.

To begin to investigate the role of the C1:G12 base pair in the Mg^{2+}-dependent aggregation of TL-II, we replaced G12 with 2′-dG12. This substitution, which results in specific deletion of the 2′-hydroxyl of G12, causes the RNA to migrate as a compact band slightly

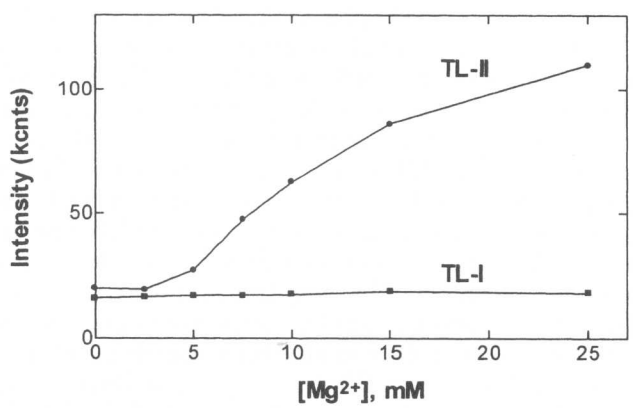

FIG. 5. Plot of the raw scattering intensities from the G1:C12 sample (TL-I) and C1:G12 sample (TL-II) as a function of added $MgCl_2$. The data plotted here were obtained at a scattering angle of 90°. The intensity values are given in the units of kilophoton counts per second (kcnt/s).

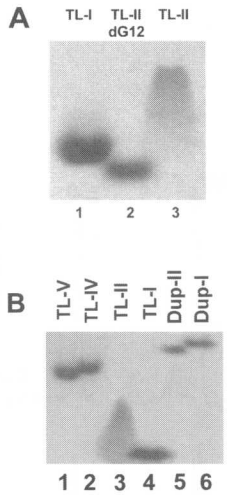

FIG. 6. (A) Native polyacrylamide gel electrophoresis of TL-I (lane 1), dG12-TL-II (lane 2), and TL-II (lane 3). (B) Effect of helical stem on native gel mobility of small RNAs. Lane 1, TL-V; lane 2, TL-IV; lane 3, TL-II; lane 4, TL-I; lane 5, Dup-II; lane 6, Dup-I. Electrophoresis was at 25°C in the presence of 10 mM $MgCl_2$ with 190 μM (20 μg in 20 μL) RNA loaded per lane. RNA was visualized by UV-shadowing.

faster than TL-I (Fig. 6A, lane 2). Therefore, the aggregation of TL-II depends on the 2′-hydroxyl at position 12 in addition to the presence of Mg^{2+} (Fig. 2).

The TL-I and TL-II sequences both have a G:U pair at the third position of the helix. Substitution of G:C at this position in TL-II (Fig. 1, TL-III) also resulted in an RNA that migrated as a smeared band on a native gel, similar to TL-II (data not shown). Therefore, the aggregation does not depend on the presence of a wobble base pair at the third position.

To determine the effect of the length of the helical stem on these observations, we prepared RNA hairpins with three additional base pairs inserted between G3:U10 and the closing base pair of the tetraloop. We analyzed both G1:C18 (Fig. 1, TL-IV) and C1:G18 (Fig. 1, TL-V) variants in this context. In contrast to the shorter hairpins (Fig. 6B, lanes 3 and 4), the RNAs with longer helices essentially comigrated as single compact bands at high concentrations and in the presence of Mg^{2+} (Fig. 6B, lanes 1 and 2). In particular, no aggregation of the C1:G18 variant was observed. The slightly increased migration of the C1:G18 variant (TL-V) is presumably due to differences in stacking of the single-stranded A19 over the first base pair (see below). We observed a similar result in a comparison of the native gel migration of nine base pair duplexes that did not contain a loop (Fig. 1, Dup-I and Dup-II), but that had similar sequences to TL-IV and TL-V (Fig. 6B, lanes 5 and 6). Thus, the length of the stem appears to be an important factor in the aggregation phenomenon. Based on these experiments, we cannot rule out the possibility that the identity of the fourth base pair, which is C:G in the shorter hairpins and G:C in the longer variants, also contributes to the observed behavior.

To further explore the RNA sequence elements responsible for TL-II aggregation, we designed a series of native gel electrophoresis experiments using variants of both hairpins. First, we analyzed truncated hairpin samples prepared without the single-stranded ACCA-3′ overhang. The two truncated hairpins (12-mer) migrated similarly on a native gel in the presence of Mg^{2+} (Fig. 7, lanes 1 and 10). We also synthesized hairpins with A-3′, AC-3′, and ACC-3′ overhangs (13-, 14-, and 15-mer, respectively). These variants were analyzed on the same native gel as the 12-mer and full-length 16-mer hairpins. Upon addition of A13 (13-mer), the distance that the two samples migrated differed slightly, apparently due to differences in stacking a 3′-purine onto a closing G:C versus a C:G base pair (Fig. 7, lane 2 versus lane 9). After addition of each of the next two C residues, the two RNAs essentially comigrated in the native gel (Fig. 7, lanes 3 versus 8, and lane 4 versus lane 7). Only when the last adenosine residue (A16) was present at the 3′ terminus was the large difference in migration between the G1:C12 and C1:G12 variants observed (Fig. 7, lane 5 versus lane 6). This experiment shows that the presence of A16 somehow induces the aggregation of the C1:G12-containing hairpin.

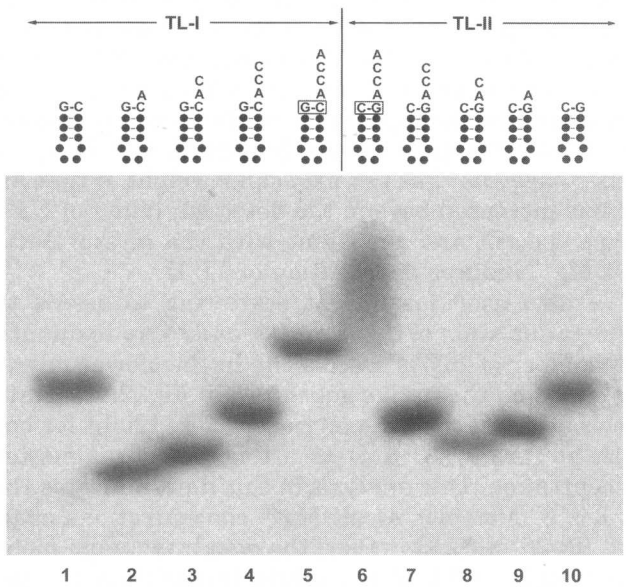

FIG. 7. Native polyacrylamide gel electrophoresis of full-length and truncated hairpin variants. The sequence of each hairpin is shown above each lane, with black dots representing nucleotides conserved in each variant (see Fig. 1). Lanes 1 and 10, 12-mer; lanes 2 and 9, 13-mer; lanes 3 and 8, 14-mer; lanes 4 and 7, 15-mer; lanes 5 and 6, 16-mer. Electrophoresis was at 20°C in the presence of 10 mM $MgCl_2$ with 190–250 μM (20 μg in 20 μL) RNA loaded per lane. RNA was visualized by UV-shadowing.

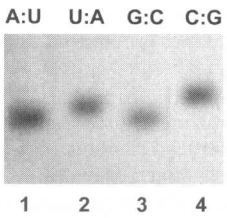

FIG. 8. Electrophoresis of 13-mer RNA sequence variants analogous to those run in lanes 2 and 9 in Fig. 7. Lane 1, A1:U12; lane 2, U1:A12; lane 3, G1:C12; lane 4, C1:G12. Electrophoresis conditions were the same as those in Fig. 7.

Figure 7 also shows that native gel electrophoresis appears to be a very sensitive probe of sequence-dependent stacking differences at the ends of helices. The 13-mer containing a G1:C12 base pair (lane 2) migrates significantly faster than the C1:G12-containing 13-mer (lane 9). Both of the RNAs end with a 3′-A single base overhang. Similar differences are observed for 13-mer containing A:U versus U:A terminal base pairs and a 3′-A overhang (Fig. 8).

DISCUSSION

Divalent metal ions are an important physiological component of folded RNAs *in vivo* and can induce both subtle and dramatic changes in RNA structure *in vitro* (1, 14–20). For example, Lilley and co-workers have shown that there is a specific backbone 2′-hydroxyl and base requirement at position G5 for proper magnesium ion-dependent folding of the hammerhead ribozyme into an active conformation (1). It should be noted that RNAs containing the UUCG tetraloop used in the studies reported here have not been shown to associate via loop–loop interactions (21, 22). While it is of interest to include metal ions in structural analyses of RNA, divalent ions often induce RNA aggregation, especially at the high RNA concentrations required for solution NMR or crystallography studies. In our study, the Mg^{2+}-induced structural heterogeneity and apparent aggregation of TL-II, which we first observe using a native gel assay and one-dimensional solution NMR, was confirmed to be aggregation using laser light scattering techniques. While structural details remain unknown, we show that specific sequence elements (including the 3′-terminal A16 and the 2′-hydroxyl of G12) and magnesium influence the tendency of RNA TL-II to adopt different aggregation states. Our study of small RNA hairpins supports the notion that even subtle changes in base or backbone composition can induce (or prevent) magnesium-dependent structural heterogeneity and aggregation of RNAs.

Previous studies have also demonstrated that the stability of RNA–RNA interactions does not vary simply with the number of Watson–Crick base pairs that can form, but depends on other factors such as base stacking effects (23–25). According to nearest neighbor free energy parameters (24, 26), the G1:C12 13-mer derived from TL-I, which contains a 3′-A single base overhang, is predicted to have greater stability than the analogous C1:G12 variant ($\Delta\Delta G$ = 1.5 kcal/mol). This difference is significant, and is presumably due to more favorable stacking of a 3′-A over the terminal G1:C12 base pair. Our analysis shows that native gel electrophoresis is sensitive to conformational variations apparently caused by subtle 3′-base stacking differences (Figs. 6B, 7, and 8). A recent high-resolution NMR structure of microhelix^{Ala} (Fig. 1, TL-IV) predicts a stacking interaction in which A73 (analogous to A19 in TL-IV) stacks over G1 on the opposite strand (27). Although the structure of the C1:G18 variant (Fig. 1, TL-V) is unknown, based on our gel electrophoresis analysis, differences in 3′-base stacking interactions are predicted relative to those observed in TL-IV. Molecular dynamics simulations and NMR studies are currently underway to further define the structural differences between these RNAs.

ACKNOWLEDGMENTS

We are grateful to Dr. Letitia Yao for assistance with the NMR experiments. We thank Dr. Caroline Kriss and Professors Victor Bloomfield and L. James Maher for helpful suggestions and critical reading of the manuscript. This work was supported by National Institutes of Health Grant GM49928 and an American Chemical Society–Petroleum Research Fund grant to K.M.F. P.J.B. received support from National Institutes of Health Molecular Biophysics Training Grant GM08277. M.R.T. was supported by a fellowship from the American Foundation for Pharmaceutical Education. All of the authors thank the University of Minnesota Graduate School for funding the Nucleic Acids Interdisciplinary Group.

REFERENCES

1. Bassi, G. S., Murchie, A. I. H., and Lilley, D. M. J. (1996) The ion-induced folding of the hammerhead ribozyme: Core sequence changes that perturb folding into the active conformation. *RNA* **2,** 756–768.
2. Maniatis, T., Fritsch, E. F., and Sambrook, J. (1982) Molecular Cloning: A Laboratory Manual, Cold Spring Harbor Laboratory Press, Cold Spring Harbor, NY.
3. Scaringe, S. A., Francklyn, C., and Usman, N. (1990) Chemical synthesis of biologically active oligoribonucleotides using β-cyanoethyl protected ribonucleoside phosphoramidites. *Nucleic Acids Res.* **18,** 5433–5441.
4. Sproat, B., Colonna, F., Mullah, B., Tsou, D., Andrus, A., Hampel, A., and Vinayak, R. (1995) An efficient method for the isolation and purification of oligoribonucleotides. *Nucleosides Nucleotides* **14,** 255–273.
5. Liu, H., and Musier-Forsyth, K. (1994) *Escherichia coli* proline tRNA synthetase is sensitive to changes in the core region of tRNA^{Pro}. *Biochemistry* **33,** 12708–12714.
6. Northrop, T. G., Nutter, R. L., and Sinsheimer, R. L. (1953) Refractive increment of thymus nucleic acid. *J. Am. Chem. Soc.* **75,** 5134–5135.
7. Varani, G., Cheong, C., and Tinoco, I., Jr. (1991) Structure of an unusually stable RNA hairpin. *Biochemistry* **30,** 3280–3289.

8. Limmer, S., Hofmann, H.-P., Ott, G., and Sprinzl, M. (1993) The 3′-terminal end (NCCA) of tRNA determines the structure and stability of the aminoacyl acceptor stem. *Proc. Natl. Acad. Sci. USA* **90,** 6199–6202.
9. Allain, F. H.-T., and Varani, G. (1995) Structure of the P1 helix from group I self-splicing introns. *J. Mol. Biol.* **250,** 330–353.
10. Limmer, S., Reif, B., Ott, G., Lubos, A., and Sprinzl, M. (1996) NMR evidence for helix geometry modifications by a G-U wobble base pair in the acceptor arm of *E. coli* $tRNA^{Ala}$. *FEBS Lett.* **385,** 15–20.
11. Liu, H., Kessler, J., Peterson, R., and Musier-Forsyth, K. (1995) Evidence for class-specific discrimination of a semiconserved base pair by tRNA synthetases. *Biochemistry* **34,** 9795–9800.
12. Shi, J.-P., Martinis, S. A., and Schimmel, P. (1992) RNA tetraloops as minimalist substrates for aminoacylation. *Biochemistry* **31,** 4931–4936.
13. Ott, G., Arnold, L., and Limmer, S. (1993) Proton NMR studies of manganese ion binding to tRNA-derived acceptor stem duplexes. *Nucleic Acids Res.* **21,** 5859–5864.
14. Leontis, N. B., Ghosh, P., and Moore, P. B. (1986) Effect of magnesium ion on the structure of the 5S RNA from *Escherichia coli.* An imino proton magentic resonance study of helix I, IV, and V regions of the molecule. *Biochemistry* **25,** 7386–7392.
15. Wyatt, J. R., Puglisi, J. D., and Tinoco, I., Jr. (1990) RNA pseudoknots: Stability and loop requirements. *J. Mol. Biol.* **214,** 455–470.
16. Chen, Y., Sierzputowska-Gracz, H., Guenther, R., Everett, K., and Agris, P. F. (1993) 5-Methylcytidine is required for cooperative binding of Mg^{2+} and a conformational transition at the anticodon stem-loop of yeast phenylalanine tRNA. *Biochemistry* **32,** 10249–10253.
17. Cate, J. H., and Doudna, J. A. (1996) Metal-binding sites in the major groove of a large ribozyme domain. *Structure* **4,** 1221–1229.
18. Rastogi, T., Beattie, T. L., Olive, J. E., and Collins, R. A. (1996) A long-range pseudoknot is required for activity of the *Neurospora* VS ribozyme. *EMBO J.* **15,** 2820–2825.
19. Scott, W. G., Murray, J. B., Arnold, J. R. P., Stoddard, B. L., and Klug, A. (1996) Capturing the structure of a catalytic RNA intermediate: The hammerhead ribozyme. *Science* **274,** 2065–2069.
20. Chen, C., and Guo, P. (1997) Magnesium-induced conformational change of packaging RNA for procapsid recognition and binding during phage ϕ29 DNA encapsidation. *J. Virol.* **71,** 495–500.
21. Kirchner, R., Vogtherr, M., Limmer, S., and Sprinzl, M. (1998) Secondary structure dimorphism and interconversion between hairpin and duplex forms of oligoribonucleotides. *Antisense Nucleic Acid Drug Dev.* **8,** 507–516.
22. Leulliot, N., Baumruk, V., Abdelkafi, M., Turpin, P.-Y., Namane, A., Gouyette, C., Huynh-Dunh, T., and Ghomi, M. (1999) Unusual nucleotide conformations in GNRA and UNCG type tetraloop hairpins: Evidence from Raman markers assignments. *Nucleic Acids Res.* **27,** 1398–1404.
23. Freier, S. M., Alkema, D., Sinclair, A., Neilson, T., and Turner, D. H. (1985) Contributions of dangling end stacking and terminal base-pair formation to the stabilities of XGGCCp, XCCGGp, XGGCCYp, and XCCGGYp helixes. *Biochemistry* **24,** 4533–4539.
24. Turner, D. H., Sugimoto, N., and Freier, S. M. (1988) RNA structure prediction. *Ann. Rev. Biophys. Biophys. Chem.* **17,** 167–192.
25. Gregorian, R. S., Jr., and Crothers, D. M. (1995) Determinants of RNA hairpin loop-loop complex stability. *J. Mol. Biol.* **248,** 968–984.
26. Sugimoto, N., Kierzek, R., and Turner, D. H. (1987) Sequence dependence for the energetics of dangling ends and terminal base pairs in ribonucleic acid. *Biochemistry* **26,** 4554–4558.
27. Ramos, A., and Varani, G. (1997) Structure of the acceptor stem of *Escherichia coli* $tRNA^{Ala}$: Role of the G3:U70 base pair in synthetase recognition. *Nucleic Acids Res.* **25,** 2083–2090.